NUCLEAR THEORY, Vol. 31 (2012)
eds. A. Georgieva, N. Minkov, Heron Press, Sofia

Internal Structure and Composition of Magnetar Crusts with Hartree-Fock-Bogoliubov Atomic Mass Models

N. Chamel[1], **R. L. Pavlov**[2], **L. M. Mihailov**[3], **Ch. J. Velchev**[2], **Zh. K. Stoyanov**[2], **Y. D. Mutafchieva**[2], **M. D. Ivanovich**[2]

[1]Institute of Astronomy and Astrophysics, Université Libre de Bruxelles, CP 226, Boulevard du Triomphe, B-1050 Brussels, Belgium

[2]Institute for Nuclear Research and Nuclear Energy, Bulgarian Academy of Sciences, 72 Tsarigradsko Chaussee, 1784 Sofia, Bulgaria

[3]Institute of Solid State Physics, Bulgarian Academy of Sciences, 72 Tsarigradsko Chaussee, 1784 Sofia, Bulgaria

Abstract. The internal structure of the outer crust of cold non-accreting magnetars has been determined for different magnetic field strengths in the framework of the magnetic BPS model. We have made use of the most recent experimental atomic mass data complemented with a microscopic atomic mass model based on the Hartree-Fock-Bogoliubov method.

1 Introduction

Born from the catastrophic gravitational core collapse of stars with a mass $M \gtrsim 8M_\odot$ during type II supernova explosions, neutron stars are among the most compact objects in the universe (see *e.g.* [1]). Their central density can exceed several times the density encountered in the heaviest atomic nuclei. Neutron stars are also the most strongly magnetized objects. Whereas most pulsars are endowed with typical surface magnetic fields of order 10^{12} G, Duncan and Thompson showed that much stronger magnetic fields up to $\sim 10^{16} - 10^{17}$ G could be generated via dynamo effects in hot newly-born neutron stars with initial periods of a few milliseconds [2]. Soft gamma-ray repeaters and anomalous X-ray pulsars are believed to be the best candidates of these so called magnetars (see *e.g.* [3] for a review). Their surface magnetic fields are estimated to be of order $10^{14} - 10^{15}$ G assuming that their spin-down is due to magnetic dipole radiation (see *e.g.* [4]). According to the virial theorem, their internal magnetic field could reach 10^{18} G [5] (neutron stars would be disrupted by stronger fields). This limit has been confirmed by numerical magnetohydrodynamics simulations [6–8].

The interior of a neutron star is composed of four main regions: i) the outer crust primarily composed of pressure ionized atoms arranged in a regular crystal lattice and embedded in a highly degenerate electron gas [9], ii) the inner crust

at densities $\gtrsim 4 \times 10^{11}$ g/cm^3 where nuclei coexist with a neutron liquid [10], iii) the outer core at densities above $\sim 10^{14}$ g/cm^3 made of a uniform mixture of nucleons and leptons, and iv) the inner core whose composition remains very uncertain [11, 12].

In a previous work, we studied the impact of a strongly quantizing magnetic field on the outer crust of a neutron star [13]. We have recently extended this analysis to lower magnetic field strengths and we have performed systematic calculations of the internal structure of the outer crust of a magnetar [14] (for a study of the denser regions of a magnetar, see *e.g.* [15–17]). In Section 2, we review the microscopic model used to describe the outer crust. Results are discussed in Section 3.

2 Microscopic Model of Magnetar Crusts

We have determined the composition of the outer crust of a magnetar using the magnetic BPS model of Ref. [5]. The outer crust is assumed to be made of fully ionised atoms arranged in a body-centered cubic lattice at zero temperature. In addition, the outer crust is supposed to contain homogeneous crystalline structures, *i.e.*structures made of only one type of nuclides with proton number Z and atomic number A. The values of Z and A in each layer of pressure P are found by minimising the Gibbs free energy per nucleon

$$g = \frac{\mathcal{E} + P}{n} \tag{1}$$

with n the average nucleon number density and $\mathcal{E}$ the average energy density given by

$$\mathcal{E} = n_N M'(Z, A) + \mathcal{E}_e + \mathcal{E}_L \tag{2}$$

where $n_N = n/A$ is the number density of nuclei, $M'(Z, A)$ their mass (including the rest mass of nucleons and Z electrons), $\mathcal{E}_e$ the energy density of electrons after subtracting out the electron rest mass energy density and $\mathcal{E}_L$ the lattice energy density. The nuclear mass $M'(Z, A)$ can be obtained from the atomic mass $M(Z, A)$ after substracting out the binding energy of the atomic electrons (see *e.g.* [9]). As in Ref. [5], we will ignore the change of nuclear masses caused by the magnetic field. According to recent fully self-consistent relativistic mean-field calculations [18], magnetic field strengths $B \lesssim 10^{17}$ G do not have any substantial impact on nuclear masses and therefore on the composition of the outer crust. We have made use of the most recent experimental atomic mass data from a preliminary unpublished version of an updated Atomic Mass Evaluation (AME) [19]. For the masses that have not yet been measured, we have employed the microscopic atomic mass model HFB-21 of Ref. [20] based on the Hartree-Fock-Bogoliubov method (see *e.g.* [21] for a review). This model was found to yield an excellent fit to the most recent atomic mass measurements [22].

In the presence of a strong magnetic field, the electron motion perpendicular to the field is quantized into Landau levels (see e.g. Chapter 4 of Ref. [1]). We

will neglect the small electron anomalous magnetic moment and electron polarization effects (see e.g. Chapter 4 of Ref. [1] and references therein). Treating electrons as a relativistic Fermi gas, the energies of Landau levels are given by [23]

$$e_\nu = \sqrt{c^2 p_z^2 + m_e^2 c^4 (1 + 2\nu B_\star)} \tag{3}$$

$$\nu = n_L + \frac{1}{2} + \sigma \,, \tag{4}$$

where n_L is any non-negative integer, $\sigma = \pm 1/2$ is the spin, p_z is the component of the momentum along the field, and the magnetic field $B_\star = B/B_c$ is measured in units of the critical magnetic field

$$B_c = \frac{m_e^2 c^3}{e\hbar} \simeq 4.4 \times 10^{13}\,\mathrm{G}\,. \tag{5}$$

In our previous study [13], we considered only strongly quantizing magnetic fields for which only the lowest level $\nu = 0$ is filled. For the HFB-21 atomic mass model, we have found that this situation occurs in any layer of the outer crust provided $B_\star > 1304$. However for lower fields, the number of occupied Landau levels can become very large, as shown in Table 1. In this work, we have therefore included the contribution of all Landau levels.

Table 1. Number of occupied Landau levels at neutron drip

$B_\star$	1000	500	100	50	10	1
$\nu_{\max}$	2	3	14	28	137	1365

For a given magnetic field $B_\star$, the number of occupied Landau levels is determined by the electron number density n_e

$$n_e = \frac{2B_\star}{(2\pi)^2 \lambda_e^3} \sum_{\nu=0}^{\nu_{\max}} g_\nu x_e(\nu)\,, \tag{6}$$

$$x_e(\nu) = \sqrt{\gamma_e^2 - 1 - 2\nu B_\star}\,, \tag{7}$$

where $\lambda_e = \hbar/m_e c$ is the electron Compton wavelength, γ_e is the electron chemical potential in units of the electron rest mass energy, i.e.

$$\gamma_e = \frac{\mu_e}{m_e c^2}\,, \tag{8}$$

while the degeneracy g_ν is $g_\nu = 1$ for $\nu = 0$ and $g_\nu = 2$ for $\nu \geq 1$.

The electron energy density $\mathcal{E}_e$ and corresponding electron pressure P_e are given by (see *e.g.* [5] and references therein)

$$\mathcal{E}_e = \frac{B_\star m_e c^2}{(2\pi)^2 \lambda_e^3} \sum_{\nu=0}^{\nu_{\max}} g_\nu (1 + 2\nu B_\star) \psi_+ \left[\frac{x_e(\nu)}{\sqrt{1 + 2\nu B_\star}} \right] - n_e m_e c^2\,, \tag{9}$$

and

$$P_e = \frac{B_\star m_e c^2}{(2\pi)^2 \lambda_e^3} \sum_{\nu=0}^{\nu_{\max}} g_\nu (1+2\nu B_\star) \psi_- \left[\frac{x_e(\nu)}{\sqrt{1+2\nu B_\star}} \right], \tag{10}$$

respectively, where

$$\psi_\pm(x) = x\sqrt{1+x^2} \pm \ln(x+\sqrt{1+x^2}). \tag{11}$$

In the absence of magnetic fields, the electron energy density and pressure reduce to (see *e.g.* Chapter 2 in [1])

$$\mathcal{E}_e = \frac{m_e c^2}{8\pi^2 \lambda_e^3} \left[x_r (1+2x_r^2)\sqrt{1+x_r^2} - \ln(x_r+\sqrt{1+x_r^2}) \right] - n_e m_e c^2, \tag{12}$$

and

$$P_e = \frac{m_e c^2}{8\pi^2 \lambda_e^3} \left[x_r \left(\frac{2}{3} x_r^2 - 1 \right) \sqrt{1+x_r^2} + \ln(x_r+\sqrt{1+x_r^2}) \right], \tag{13}$$

respectively, where $x_r = \hbar (3\pi^2 n_e)^{1/3}/(m_e c)$ is the relativity parameter.

According to the Bohr-van Leeuwen theorem [24, 25], the lattice energy density is not affected by the magnetic field. We use the same expression as in [13] and we neglect the small contribution due to quantum zero-point motion of ions [26].

Collecting all terms, the Gibbs free energy per nucleon (1) can be equivalently written as

$$g = \frac{M'(A,Z)}{A} + \frac{Z}{A} \left(\mu_e - m_e c^2 + \frac{4}{3} \frac{\mathcal{E}_L}{n_e} \right). \tag{14}$$

Note that at equilibrium, the neutron chemical potential is simply given by $\mu_n = \mu_p + \mu_e$, where μ_p is the proton chemical potential. Using electric charge neutrality $n_e = n_p$ and the identity

$$n g = n_n \mu_n + n_p \mu_p + n_e \mu_e, \tag{15}$$

where $n = n_n + n_p$, we conclude that the value of g at equilibrium is simply equal to the neutron chemical potential. Consequently, at the bottom of the crust where neutrons drip out of nuclei, the Gibbs free energy per nucleon is given by $g = \mu_n = m_n c^2$ (m_n being the neutron mass).

3 Internal Composition of Magnetar Crusts

We have determined the composition of cold non-accreting magnetar crusts for different magnetic field strengths. Results are summarized in Table 2. We have found that the sequence of equilibrium nuclides is not affected by the magnetic field for $B_\star \lesssim 1$, as in most radio pulsars. However the highest pressure at which

Table 2. Sequence of equilibrium nuclides with increasing depth in the outer crust of a cold non-accreting neutron star for different magnetic field strengths. The nuclides with experimentally measured masses are indicated in boldface.

$B_\star = 0$	$B_\star = 1$	$B_\star = 10$	$B_\star = 100$	$B_\star = 1000$	$B_\star = 2000$
^{56}**Fe**	^{56}**Fe**	^{56}**Fe**	^{56}**Fe**	^{56}**Fe**	^{56}**Fe**
^{62}**Ni**	^{62}**Ni**	^{62}**Ni**	^{62}**Ni**	^{62}**Ni**	^{62}**Ni**
^{58}**Fe**	^{58}**Fe**	–	–	–	–
^{64}**Ni**	^{64}**Ni**	^{64}**Ni**	^{64}**Ni**	^{64}**Ni**	–
^{66}**Ni**	^{66}**Ni**	^{66}**Ni**	–	–	–
–	–	–	–	^{88}**Sr**	^{88}**Sr**
^{86}**Kr**	^{86}**Kr**	^{86}**Kr**	^{86}**Kr**	^{86}**Kr**	^{86}**Kr**
^{84}**Se**	^{84}**Se**	^{84}**Se**	^{84}**Se**	^{84}**Se**	^{84}**Se**
^{82}**Ge**	^{82}**Ge**	^{82}**Ge**	^{82}**Ge**	^{82}**Ge**	^{82}**Ge**
–	–	–	–	–	^{132}**Sn**
^{80}**Zn**	^{80}**Zn**	^{80}**Zn**	^{80}**Zn**	^{80}**Zn**	^{80}**Zn**
–	–	–	–	–	^{130}**Cd**
–	–	–	–	–	^{128}Pd
–	–	–	–	–	^{126}Ru
^{79}Cu	^{79}Cu	^{79}Cu	^{79}Cu	^{79}Cu	–
^{78}Ni	^{78}Ni	^{78}Ni	^{78}Ni	^{78}Ni	–
^{80}Ni	^{80}Ni	^{80}Ni	^{80}Ni	^{80}Ni	–
^{124}Mo	^{124}Mo	^{124}Mo	^{124}Mo	^{124}Mo	^{124}Mo
^{122}Zr	^{122}Zr	^{122}Zr	^{122}Zr	^{122}Zr	^{122}Zr
^{121}Y	^{121}Y	^{121}Y	^{121}Y	^{121}Y	^{121}Y
^{120}Sr	^{120}Sr	^{120}Sr	^{120}Sr	^{120}Sr	^{120}Sr
^{122}Sr	^{122}Sr	^{122}Sr	^{122}Sr	^{122}Sr	^{122}Sr
^{124}Sr	^{124}Sr	^{124}Sr	^{124}Sr	^{124}Sr	^{124}Sr

each nuclide can be found is increased, especially in the shallow region of the outer crust where the effects of Landau quantization are the most important. For example, the maximum pressure at which ^{56}Fe is present, is raised from 3.36×10^{-10} MeV fm^{-3} for $B_\star = 0$ to 4.15×10^{-10} MeV fm^{-3} for $B_\star = 1$. Note that for $B_\star = 0$ the outer crust is found to contain ^{58}Fe whereas it was not predicted in [9] using the same HFB-21 atomic mass model. This is because we have neglected electron exchange and other small corrections that were included in [9]. For the strong fields $B_\star \gg 1$ expected to prevail in the interior of magnetars, the sequence of equilibrium nuclides exhibits significant deviations compared to that obtained for $B_\star = 0$. In addition, such strong magnetic fields tend to prevent neutrons from dripping out of nuclei. As a result, the pressure at the neutron drip transition is increased even though the corresponding equilibrium nuclide does not change.

As shown in Figures 1 and 2, the differences in the Gibbs free energy per nucleon around the equilibrium configuration are very small. For example, the equilibrium nuclide at the pressure $P = 1.1 \times 10^{-5}$ MeV fm^{-3} and for

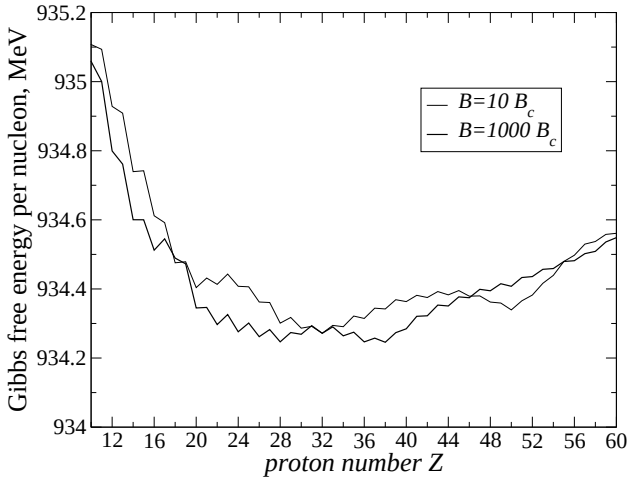

Figure 1. Gibbs free energy per nucleon g as a function of the proton number Z in the outer crust of a cold non-accreting neutron star with a magnetic field $B_\star = 1000$ (thick line) and with $B_\star = 10$ (thin line) at the same pressure $P = 1.1 \times 10^{-5}$ MeV fm^{-3}. The Gibbs free energy per nucleon for $B_\star = 1000$ was shifted so that it yields the same value for $Z = 32$ as that obtained for $B_\star = 10$.

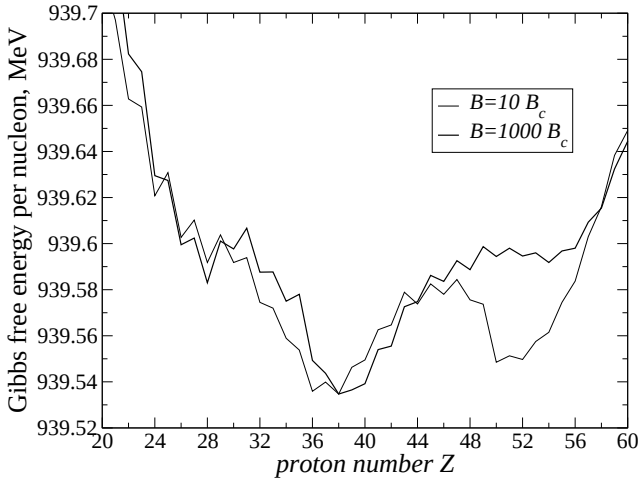

Figure 2. Gibbs free energy per nucleon g as a function of the proton number Z in the outer crust of a cold non-accreting neutron star with a magnetic field $B_\star = 1000$ (thick line) and with $B_\star = 10$ (thin line) at the same pressure $P = 4.8 \times 10^{-4}$ MeV fm^{-3}. The Gibbs free energy per nucleon for $B_\star = 1000$ was shifted so that it yields the same value for $Z = 38$ as that obtained for $B_\star = 10$.

$B_\star = 1000$ is ^{88}Sr. The corresponding Gibbs free energy per nucleon is lower than that of ^{86}Kr and ^{64}Ni by respectively 1.1 keV and 1.3 keV only. Likewise, in the deeper region of the outer crust where $P = 4.8 \times 10^{-4}$ MeV fm^{-3} for $B_\star = 1000$, the Gibbs free energies per nucleon of ^{120}Sr (the equilibrium nuclide), ^{121}Y and ^{124}Zr differ by less than 4.5 keV. This suggests that the small corrections to g that we have neglected here like electron polarization may change the composition. Moreover, we anticipate that at finite temperatures the outer crust will presumably be made of heteregeneous structures, with different nuclides coexisting at the same pressure.

Because the crust of a magnetar can have a different composition from that of an ordinary pulsar, its properties can also be different. For instance, we have calculated the "effective" shear modulus S of a body-centered-cubic lattice polycrystal using the following expression from [27] :

$$S = 0.1194 n_{\rm N} \frac{Z^2 e^2}{R_{\rm N}} \,, \tag{16}$$

where $R_{\rm N}$ is the ion-sphere radius defined by

$$R_{\rm N} = \left(\frac{3}{4\pi n_{\rm N}} \right)^{1/3} . \tag{17}$$

As shown in Figure 3, the shear modulus of a magnetar can be much larger than that of an ordinary neutron star.

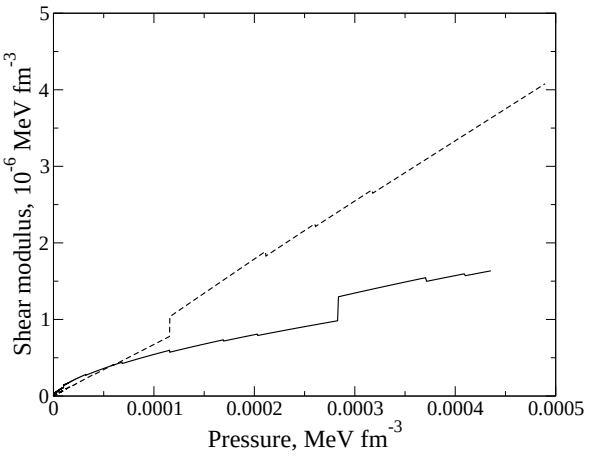

Figure 3. Effective shear modulus in the outer crust of a cold non-accreting neutron star with a magnetic field $B_\star = 1000$ (dashed line) and with $B_\star = 0$ (solid line). Note that the neutron drip pressure for $B_\star = 1000$ is higher than that for $B_\star = 0$.

4 Conclusion

We have calculated the internal composition of the outer crust of cold non-accreting magnetars using the most recent experimental atomic mass data complemented with the latest Hartree-Fock-Bogoliubov atomic mass model. The outer crust of a magnetar is found to have a substantially different composition (hence also different properties) compared to that of ordinary pulsars. In particular, the shear modulus of the outer crust is found to be enhanced by the strong magnetic field. These results may have implications for the interpretation of quasiperiodic oscillations observed in soft-gamma-ray repeaters. This warrants further studies.

Acknowledgements

The present work was supported by the bilateral project between FNRS (Belgium), Wallonie-Bruxelles-International (Belgium) and the Bulgarian Academy of Sciences. This work was also supported by CompStar, a Research Networking Programme of the European Science Foundation.

References

[1] P. Haensel, A.Y. Potekhin, D.G. Yakovlev, *Neutron Stars 1: Equation of State and Structure* (Springer, 2007).
[2] C. Thompson and R.C. Duncan, *Astrophys. J.* **408** (1993) 194.
[3] P.M. Woods, and C. Thompson, in:) *Compact Stellar X-ray Sources*, edited by W. H. G. Lewin and M. van der Klis (Cambridge University Press, Cambridge, 2006) 547.
[4] McGill SGR/AXP Online Catalog, URL: `http://www.physics.mcgill.ca/~pulsar/magnetar/main.html` [cited 30 August 2011].
[5] D. Lai and S.L. Shapiro, *Astrophys. J.* **383** (1991) 745.
[6] M. Bocquet, S. Bonazzola, E. Gourgoulhon, J. Novak, *Astron. Astrophys*. **301** (1995) 757.
[7] C.Y. Cardall, M. Prakash, J.M. Lattimer, *Astrophys. J.* **554** (2001) 322.
[8] K. Kiuchi and K. Kotake, *Month. Not. Roy. Astr. Soc*. **385** (2008) 1327.
[9] J.M. Pearson, S. Goriely, and N. Chamel, *Phys. Rev. C* **83** (2011) 065810.
[10] J.M. Pearson, N. Chamel, S. Goriely, and C. Ducoin, *Phys. Rev. C* **85** (2012) 065803.
[11] D. Page and S. Reddy, *Annu. Rev. Nucl. Part. Sci*. **56** (2006) 327.
[12] F. Weber, R. Negreiros, P. Rosenfield, and M. Stejner, *Prog. Part. Nucl. Phys*. **59** (2007) 94.
[13] N. Chamel, R.L. Pavlov, L.M. Mihailov, Ch.J. Velchev, Zh.K. Stoyanov, Y.D. Mutafchieva, M.D. Ivanovich, in: *Proceedings of the XXX International Workshop on Nuclear Theory, Rila Mountains, Bulgaria, 26 June – 2 July 2011*, edited by A. Georgieva and N. Minkov (Heron Press, Sofia, 2011) 240-246.
[14] N. Chamel, R.L. Pavlov, L.M. Mihailov, Ch.J. Velchev, Zh.K. Stoyanov, Y.D. Mutafchieva, M.D. Ivanovich, J.M. Pearson, S. Goriely, submitted to *Phys. Rev. C*.

[15] R. Nandi, D. Bandyopadhyay, I.N. Mishustin, W. Greiner, *Astrophys. J.* **736** (2011) 156.

[16] A. Broderick, M. Prakash, J.M. Lattimer, *Astrophys. J.* **537** (2001) 351.

[17] I.S. Suh, G.J. Mathews, *Astrophys. J.* **546** (2001) 1126.

[18] D. Peña Arteaga, M. Grasso, E. Khan, P. Ring, *Phys. Rev. C* **84** (2011) 045806.

[19] G. Audi, M. Wang, A.H. Wapstra, B. Pfeiffer, and F.G. Kondev, private communication.

[20] S. Goriely, N. Chamel, and J.M. Pearson, *Phys. Rev. C* **82** (2010) 035804.

[21] N. Chamel, S. Goriely, J.M. Pearson, in: *Proceedings of the XXVIII International Workshop on Nuclear Theory, Rila Mountains, Bulgaria, 22-27 June 2009*, edited by S. Dimitrova (Sofia, 2009) 247-253.

[22] N. Chamel, A.F. Fantina, J.M. Pearson, and S. Goriely, *Phys. Rev. C* **84** (2011) 062802(R).

[23] I.I. Rabi, *Z. Phys.* **49** (1928) 507.

[24] J.A. van Leeuwen, *J. Phys. Radium* **2** (1921) 361.

[25] J.H. Van Vleck, *the Theory of Electric and Magnetic Susceptibilities* (Oxford University Press, London, 1932).

[26] D.A. Baiko, *Phys. Rev. E* **80** (2009) 046405.

[27] S. Ogata and S. Ichimaru, *Phys. Rev. A* **42** (1990) 4867.